J|A|C|S ARTICLES

Published on Web 06/12/2009

Stabilization of Three-Way Junctions of DNA under Molecular Crowding Conditions

Sanjukta Muhuri,[†] Kenta Mimura,[‡] Daisuke Miyoshi,[†,‡] and Naoki Sugimoto*[,†,‡]

FIBER (Frontier Institute for Biomolecular Engineering Research) and FIRST (Faculty of Frontiers of Innovative Research in Science and Technology), Konan University, 7-1-20 Minatojima-Minamimachi, Chuo-ku, Kobe 650-0047, Japan

Received January 30, 2009; E-mail: sugimoto@konan-u.ac.jp

Abstract: We examined the effects of molecular crowding conditions on the structures and thermodynamics of three-way junctions (TWJs) of DNA. Structural analysis utilizing gel electrophoresis and circular dichroism spectroscopy showed that the designed DNAs folded into TWJ structures in the presence of Na^+ and Mg^{2+} under both dilute and molecular crowding conditions with polyethylene glycol 200 (PEG 200). From the thermodynamic parameters evaluated by UV melting techniques in the absence and presence of 5 mM Mg^{2+} under dilute and molecular crowding conditions, it was clear that Mg^{2+} stabilized all TWJs under the dilute condition, although the extent of stabilization depended on the stacking partners of TWJs. For example, thermodynamic stability ($-\Delta G^\circ_{37}$) of A/B-stacked TWJs (A, B, and C are the three helices of TWJ, and among these helices, A and B are stacked together) increased from 3.7 to 5.6 kcal/mol by the addition of 5 mM Mg^{2+}, while that of A/C-stacked TWJs (A and C are stacked together) increased only from 3.0 to 3.7 kcal/mol. Molecular crowding with PEG 200 destabilized the whole TWJ consisting of a junction point and three helical duplex arms. Crowding agents such as PEG 200 can affect the stability of DNA by modulating its hydration. To explore the crowding effects on the junction point, we evaluated the number of water molecules associated with the whole TWJ as well as the individual arms, and we found that the number of water molecules taken up by the whole TWJ was significantly smaller than the sum of the individual arms. These results show the dehydration from the junction point of the TWJ structure. Therefore, molecular crowding should be favorable for the junction point of TWJ structure and unfavorable for the duplex structure. To prove this concept, we designed truncated TWJ structures that folded into a bimolecular duplex under the dilute condition. With increasing concentrations of PEG 200 from 0 to 30 wt %, the fraction of truncated TWJ structures gradually increased, and that of the bimolecular duplex structure decreased, even in the absence of Mg^{2+}. We concluded that a cell-mimicking condition, in which the activity of water decreases and hydration becomes less favorable, might facilitate the formation of junction structures in comparison with duplexes.

Introduction

Junctions in nucleic acid structures arise when three or more helices meet at a single point. These branched junctions are important intermediates in many biological functions and play important roles in many cellular processes.[1] Three-way junctions (TWJs) are the simplest type of junctions and consist of three double helical arms connected at the junction point. TWJs occur both in DNA and RNA. In RNA, they are involved in splicing[2] and translation,[3] while in DNA, they are formed transiently during DNA replication (the replication fork).[4] TWJs of DNA also arise during recombination involving phages.[5] Furthermore, TWJs of DNA have been proposed to occur in the expansions of triplet repeats found in genetically unstable genomic DNA associated with human diseases such as Huntington's.[6] In addition to their roles in biological processes, branched junctions offer a unique window into DNA nanotechnology, which includes the controlled self-assembly of nanometer-scale molecular fragments.[7]

Because TWJs are the smallest type of junction structures, they are used as a model system to gain insight into other

[†] FIBER.
[‡] FIRST.

(1) (a) Kitts, P. A.; Nash, H. A. *Nature* **1987**, *329*, 346–348. (b) Orr-Weaver, T. L.; Szostak, J. W.; Rothstein, R. J. *Proc. Natl. Acad. Sci. U.S.A.* **1981**, *78*, 6354–6358.
(2) Guthrie, C.; Patterson, B. *Annu. Rev. Genet.* **1988**, *22*, 387–419.
(3) (a) Wimberly, B. T.; Brodersen, D. E.; Clemons, W. M.; Morgan-Warren, R. J.; Carter, A. P.; Vonrhein, C.; Hartsch, T.; Ramakrishnan, V. *Nature* **2000**, *407*, 327–339. (b) Ban, N.; Nissen, P.; Hansen, J.; Moore, P. B.; Steitz, T. A. *Science* **2000**, *289*, 905–920.
(4) Singleton, M. R.; Scaife, S.; Wigley, D. E. *Cell* **2001**, *107*, 79–89.
(5) Hutchins, C. J.; Rathjen, P. D.; Forster, A. C.; Symons, R. H. *Nucleic Acids Res.* **1986**, *14*, 3627–3640.
(6) (a) Jensch, F.; Kemper, B. *EMBO J.* **1986**, *5*, 181–189. (b) Minagawa, T.; Murakami, A.; Ryo, Y.; Yamagashi, H. *Virology* **1983**, *126*, 183–193. (c) Sinden, R. R. *Nature* **2001**, *411*, 757–758. (d) Cleary, J. D.; Nichol, K.; Wang, Y. H.; Pearson, C. E. *Nat. Genet.* **2002**, *31*, 37–46. (e) Pearson, C. E.; Tam, M.; Wang, Y. H.; Montgomery, S. E.; Dar, A. C.; Cleary, J. D.; Nichol, K. *Nucleic Acids Res.* **2002**, *30*, 4534–4547.
(7) (a) Seeman, N. C. *Curr. Opin. Struct. Biol* **1996**, *6*, 519–526. (b) LaBean.; H, T.; Yan, H.; Kopatsch, J.; Liu, F. R.; Winfree, E.; Rief, J. H.; Seeman, N. C. *J. Am. Chem. Soc.* **2000**, *112*, 1848–1860.

10.1021/ja900744e CCC: $40.75

complex and multibranched junction structures, such as the Holliday junction, which is a key intermediate in homologous recombination. TWJs, therefore, provide a suitable system for assessing the quantitative features of junction structures. Previous studies of three-dimensional structures and the thermodynamics of TWJs[8] have demonstrated that coaxial stacking is one of the most important conformational features of TWJs and that a divalent cation such as Mg^{2+} is critical for coaxial stacking.[9] Moreover, TWJs create a unique electrostatic environment near the junction point due to close proximity of the opposing charges. Thus, there should be larger scale changes in charge neutralization and hydration for the junction formation relative to the simple duplex.[8c] Recently, it was reported that molecular crowding, which is one of the most important cellular environmental conditions,[10] can alter the water activity leading to the hydration change.[11] The roles of water molecules in the structure and thermal stability of the TWJ can be determined by modulating the solution water activity by the addition of osmotic agents such as polyethylene glycol (PEG)[12] because PEG is the most commonly used crowding agent that is not expected to bind directly to the polynucleotides. Thus, the use of PEG as molecular crowding agent can give quantitative information that should help to explain important molecular properties under various conditions including cell mimicking, although PEG cannot make ideal replacement of the intracellular condition.

Here, we used a neutral cosolute, PEG, with the average molecular weight of 200 (PEG 200), in the absence and presence of Mg^{2+} to study systematically the effects of molecular crowding on the formation of TWJs of DNA. TWJs were stabilized considerably with the addition of 5 mM Mg^{2+} in the dilute condition and destabilized by the molecular crowding condition both in the absence and presence of 5 mM Mg^{2+}. Moreover, the destabilizing effect caused by the molecular crowding condition was for the whole TWJ structure, consisting of the junction point and three helical duplex arms. Destabilization of the whole TWJ structures under molecular crowding conditions demonstrated hydration during their formation. To reveal the crowding effect on the junction point, we estimated the numbers of water molecules taken up during the formation of the whole TWJ structure and each of the hairpin duplex arms from the slopes of linear plots of stability in terms of the equilibrium constant ($\ln K_{obs}$) of the structures versus water activity ($\ln a_w$). The differential number of water molecules taken up by the whole TWJ and each helical arm suggested that water molecules were released from the junction point. This differential hydration between the duplex and TWJ should induce the structural transition from a more hydrated duplex to the less hydrated TWJ structure under molecular crowding conditions. To prove this concept, we designed truncated DNA sequences that can form bimolecular duplexes as well as the TWJ structure under the dilute condition. We found that molecular crowding conditions were indeed able to induce the structural transition from bimolecular duplex to TWJ, even in the absence of Mg^{2+}. This finding proves that intracellular conditions, in which the water activity decreases and hydration becomes less favorable, must facilitate the formation of TWJ structures in comparison with the bimolecular duplex structure.

Experimental Section

Materials. We used high-performance liquid chromatography (HPLC) grade oligodeoxynucleotides from Hokkaido System Science (Sapporo, Japan). To determine the single-strand concentrations of the DNA oligonucleotides, we measured the absorbance at 260 nm at a high temperature by using a spectrophotometer (Shimadzu 1700; Shimadzu, Kyoto, Japan) connected to a thermoprogrammer. Single-strand extinction coefficients were calculated from mononucleotide and dinucleotide data using the nearest-neighbor approximation.[13]

Water Activity Measurements. The water activity was determined by the osmotic stressing method via vapor phase osmometry by using a pressure osmometer (model 5520XR; Wescor, Utah) with the assumption that the cosolutes do not directly interact with DNA.[14]

Circular Dichroism (CD) Measurements. A spectropolarimeter (J-820; JASCO, Hachioji, Japan) was used for CD measurements. The experiments were conducted at 4 °C with a 0.1 cm path length cuvette for 6 μM total strand concentration of DNA in buffers of 0 or 5 mM $MgCl_2$, 50 mM NaCl, 20 mM Na-cacodylate (pH 7.0), and 0.5 mM Na_2EDTA containing various concentrations of PEG 200. The CD spectra were obtained by averaging at least three scans made from 200 to 350 nm. The temperature of the cell holder was regulated by a JASCO PTC-348 temperature controller, and the cuvette-holding chamber was flushed with a constant stream of dry N_2 gas to avoid water condensation on the cuvette exterior. Before the measurement, the sample was heated to 90 °C, gently cooled at a rate of 0.5 °C min^{-1}, and incubated at 4 °C for 1 h.

Gel Electrophoresis. Native gel electrophoresis was performed on nondenaturing gels containing 15% polyacrylamide. Ice-cold loading buffer (2 μL) was mixed with 2 μL of 1 μM DNA sample in buffers of 20 mM Na-cacodylate (pH 7.0), 0.5 mM Na_2EDTA, 0 or 5 mM $MgCl_2$, and 50 mM NaCl containing various concentrations of PEG 200. A 2 μL aliquot of the mixed solution was loaded and analyzed by electrophoresis at 7.5 V cm^{-1} for 3.5 h at 4 °C. Gels were stained by using GelStar and imaged with FLA-5100 (Fuji Film Co., Ltd., Tokyo, Japan). Before the measurement, the sample was heated to 90 °C, gently cooled at a rate of 0.5 °C min^{-1}, and incubated at 4 °C for 1 h.

Thermodynamic Analysis. The UV absorbance was measured with a Shimadzu 1700 spectrophotometer equipped with a temperature controller. Melting curves for the TWJ structures were obtained by measuring the UV absorbance at 260 nm in buffers containing 20 mM Na-cacodylate (pH 7.0), 0.5 mM Na_2EDTA, 0 or 5 mM $MgCl_2$, and 50 mM NaCl supplemented with various concentrations of PEG 200. The T_m (melting temperature) values for 1 μM DNA TWJs were obtained from the UV melting curves

(8) (a) Lu, M.; Guo, Q.; Marky, L. A.; Seeman, N. C.; Kallenbach, N. R. *J. Mol. Biol.* **1992**, *223*, 781–789. (b) Ladbury, J. E.; Sturtevant, J. M.; Leontis, N. B. *Biochemistry* **1994**, *33*, 6828–6833. (c) Zhong, M.; Marky, L. A.; Kallenbach, N. R. *Biochemistry* **1997**, *36*, 2485–2491. (d) Zhong, M.; Rashes, M. S.; Leontis, N. B.; Kallenbach, N. R. *Biochemistry* **1994**, *33*, 3660–3667.

(9) (a) Welch, J. B.; Walter, F.; Lilley, D. M. J. *J. Mol. Biol.* **1995**, *251*, 507–519. (b) Leontis, N. B.; Hills, M. T.; Piotto, M.; Malhotra, A.; Nussbaum, J.; Gorenstein, D. G. *J. Biomol. Struct. Dyn.* **1993**, *11*, 215–223. (c) Rosen, M. A.; Patel, D. J. *Biochemistry* **1993**, *32*, 6563–6575.

(10) (a) Ellis, R. J.; Minton, A. P. *Nature* **2003**, *425*, 27–28. (b) Zimmerman, S. B.; Minton, A. P. *Annu. Rev. Biophys. Biomol. Struct.* **1993**, *22*, 27–65.

(11) (a) Miyoshi, D.; Karimata, H.; Sugimoto, N. *J. Am. Chem. Soc.* **2006**, *128*, 7957–7963. (b) Spink, C. H.; Chaires, J. B. *J. Am. Chem. Soc.* **1995**, *117*, 12887–12888. (c) Goobes, R.; Minsky, A. *J. Am. Chem. Soc.* **2001**, *123*, 12692–12693.

(12) Podgornic, R.; Strey, H. H.; Gawrisch, K.; Rau, D. C.; Rupprecht, A.; Parsegian, V. A. *Proc. Natl. Acad. Sci. U.S.A.* **1996**, *93*, 4261–4266.

(13) (a) Sugimoto, N.; Nakano, S.; Kotah, S.; Matsumura, A.; Nakamuta, H.; Ohmichi, T.; Yoneyama, M.; Sasaki, M. *Biochemistry* **1995**, *34*, 11211–11216. (b) Nakano, S.; Kanzaki, T.; Sugimoto, N. *J. Am. Chem. Soc.* **2004**, *126*, 1088–1095.

(14) (a) Rozners, E.; Moulder, J. *Nucleic Acids Res.* **2004**, *32*, 248–254. (b) Nakano, S.; Karimata, H.; Ohmichi, T.; Kawakami, J.; Sugimoto, N. *J. Am. Chem. Soc.* **2004**, *126*, 14330–14331.

as described previously.[13] The heating rate was 0.5 °C min^{-1} for all junctions because the shape of the melting curve and T_m were unaffected by heating rates between 0.2 and 0.5 °C min^{-1}. The thermodynamic parameters were calculated from the fit of the melting curves (with at least four different concentrations of DNA oligonucleotides) to a theoretical equation for an intramolecular association as described previously.[13,15] The thermodynamic parameters ($\Delta H°$, $\Delta S°$, and $\Delta G°_{37}$; changes of enthalpy, entropy, and Gibbs free energy for the formation of TWJs at 37 °C, respectively) are the average values obtained from the curve-fitting analyses. Before the measurement, the sample was heated to 90 °C, gently cooled at a rate of 0.5 °C min^{-1}, and incubated at 0 °C for 1 h.

Results and Discussion

Rational Design of TWJ Sequences. Most model systems for the junction structure were assembled from separate oligonucleotide strands that were annealed together to form the stable junction.[8] However, it was proposed that in many cases the melting behavior of these junction structures did not conform to the two-state model but instead involved a significant population of intermediates.[16] A two-strand RNA TWJ system, in which one of the helical arms terminated to a hairpin loop, was designed to simplify the analysis and to reduce the number of intermediates.[17] The melting temperature of the junction was well-separated from the temperature associated with the hairpin formation in the longer stand. This design demonstrates the utility of the optical melting technique to evaluate thermodynamic stability of the multibranched junction.[17] From these studies, we have designed intramolecular TWJs of DNA in which the molecularity of the system is reduced from three to one by terminating two helical arms with hairpin loops (Figure 1A). Results from NMR studies proved that the single-stranded DNA molecule can fold into an intramolecular TWJ.[18] We have chosen these sequences of intramolecular TWJs of DNA as our model systems.

Two or more unpaired nucleotides at the junction point of TWJs stabilize the structure by providing the necessary covalent bridge to allow a stacking interaction across the junction.[19] TWJs with unpaired residues at the junction point can adopt two alternative stacked conformations along with the open conformation. In the stacked conformations, two arms are coaxially stacked, such as A/B-stacked and A/C-stacked conformers (strand and arm definitions are shown in Figure 1A). On the other hand, without the unpaired nucleotides at the junction point, TWJs adopt an open conformation without coaxial stacking, even in the presence of divalent cations.[19b] Sequences around the junction point, especially the penultimate base pairs, also play a crucial role in the conformation selection process.[18a] van Buuren et al. studied the stacking behavior of 24 published TWJs to derive two empirical rules that predict the stacking preferences of the TWJs from their sequences.[20] The "pyrimidine rule" states that, in a stacked conformation, it is energetically advantageous if a pyrimidine (either C or T) in arm A is located in the crossover strand at the penultimate position (Figure 1A, penultimate positions are marked with a or b). When this pyrimidine is located at position b, A/B-stacked conformer is preferred (Figure 1A, left), whereas A/C-stacked conformer is preferred when it resides at position a (Figure 1A, right). The "loop rule" states that a thermodynamically stable quasi-hairpin loop in a specific stacking mode favors that particular conformer (Figure 1A). Therefore, a stable quasi-hairpin loop in the A/B-stacking mode ($5'$-N_4/XXN_3, Figure 1A) will favor A/B-stacked conformer, whereas a thermodynamically unstable one will not. Similarly, a stable quasi-hairpin loop in the A/C-stacking mode ($5'$-N_1XX/N_2, Figure 1A) will favor A/C-stacked conformer.

From previous findings, we constructed intramolecular TWJs of DNA that are more amenable to detailed analyses (Table 1). We selected four intramolecular TWJs (J1−J4) from previous reports.[18] These four sequences have two unpaired thymidine (TT) residues at the junction point (position marked with X−X in Figure 1A). J1 and J2 adopt an A/B-stacking conformation, whereas J3 and J4 adopt an A/C-stacking conformation according to the rules (Figure 1B,C). Sequences J5−J7 were designed by systematic changes of the base pairs near the junction point of J3 (Figure S1 in Supporting Information). To check the generality of the above rules, J8 was further designed from an intermolecular TWJ by terminating two helices with a stable CTTG hairpin loop.[8b] Sequences J9−J11 were also designed by systematic changes of the base pairs near the junction point of J8 (Figure S1 in Supporting Information).

Structural Aanalysis. The formation and stability of bulged TWJs of DNA are strongly dependent on a divalent cation like Mg^{2+}.[22] To confirm the intramolecular nature of the TWJs, we performed native gel electrophoresis of J1−J4 in the absence and presence of 5 mM Mg^{2+} and 0 or 20 wt % of PEG 200 at 4 °C with two concentrations of DNA, 1 and 30 μM (Figure 2). All sequences migrated with a single band, suggesting the formation of a unimolecular structure under all of the conditions. The migration of all TWJs was slightly faster than that of the 20 base pair band in the 10 base pair ladder marker, which is in good agreement with the 15 base pair formation of the completely folded TWJ structures. Thus, the gel electrophoresis study provided strong evidence that all of the sequences folded into stable TWJ structures under all of the conditions. Then, all TWJs were further analyzed using CD spectra. Figure 3 shows the CD spectra of four TWJs (J1−J4) at 4 °C in the absence and presence of Mg^{2+} with or without 20 wt % PEG 200. In the presence of only Na^+, all sequences showed a positive and a negative peak at 280 and 250 nm, respectively, indicating a B-like conformation (Figure 3a). Moreover, J1 and J2 had a negative peak at 210 nm, which is a signature feature for an A-like conformation, although J3 and J4 did not show such a significant negative peak near 210 nm. Thus, J1 and J2 deviated from the classical B-like conformation, whereas J3 and J4 resembled the B-like conformation. This tendency was observed for all conditions, as shown in Figure 3b−d. It was previously proven by NMR that J1 and J2 adopted the A/B-stacked

(15) (a) Marky, L. A.; Breslauer, K. J. *Biopolymers* **1987**, *26*, 1601–1620. (b) Puglisi, J. D.; Tinoco, I., Jr. *Methods Enzymol.* **1989**, *180*, 304–325.
(16) Kadrmas, J. L.; Ravin, A. J.; Leontis, N. B. *Nucleic Acids Res.* **1995**, *23*, 2212–2222.
(17) (a) Diamond, J. M.; Turner, D. H.; Mathews, D. H. *Biochemistry* **2001**, *40*, 6971–6981. (b) Mathews, D. H.; Turner, D. H. *Biochemistry* **2002**, *41*, 869–880.
(18) (a) Overmars, F. J. J.; Pikkemaat, J. A.; van den Elst, H.; van Boom, J. H.; Altona, C. *J. Mol. Biol.* **1996**, *255*, 702–713. (b) Wu, B.; Girard, F.; van Buuren, B.; Schleucher, J.; Tessari, M.; Wijmenga, S. *Nucleic Acids Res.* **2004**, *32*, 3228–3239.
(19) (a) Leontis, N. B.; Kwok, W.; Newman, J. S. *Nucleic Acids Res.* **1991**, *19*, 759–766. (b) Stuhmeier, F.; Welch, J. B.; Murchie, A. I.; Lilley, D. M. J.; Clegg, R. M. *Biochemistry* **1997**, *36*, 13530–13538. (c) Stuhmeier, F.; Lilley, D. M. J.; Clegg, R. M. *Biochemistry* **1997**, *36*, 13539–13551.
(20) van Buuren, B. N. M.; Overmars, F. J. J.; Ippel, J. H.; Altona, C.; Wijmenga, S. S. *J. Mol. Biol.* **2000**, *304*, 371–383.
(21) Altona, C. *J. Mol. Biol.* **1996**, *263*, 568–581.
(22) Welch, J. B.; Duckett, D. R.; Lilley, D. M. J. *Nucleic Acids Res.* **1993**, *21*, 4548–4555.

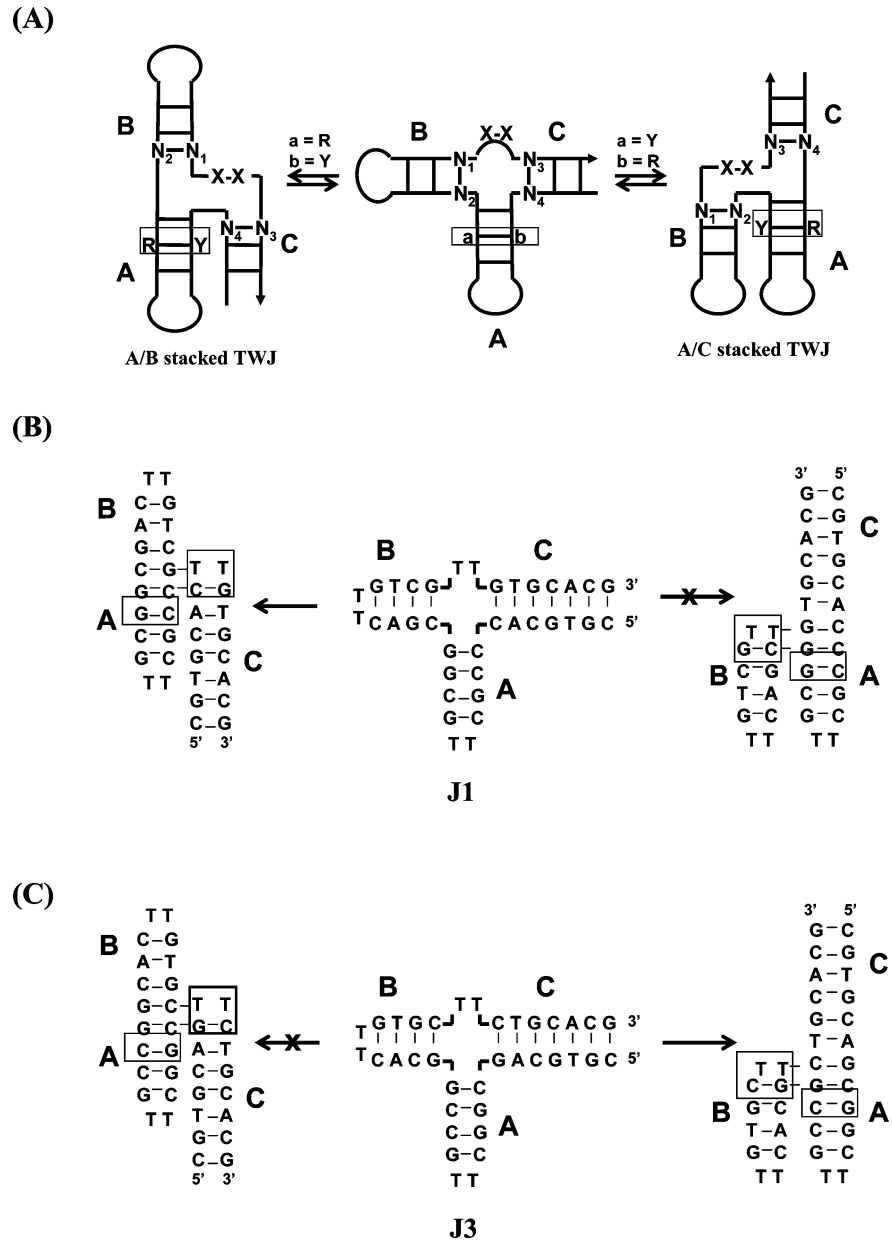

Figure 1. (A) Schematic representation of the possible conformation that can be adopted by TWJs with unpaired bases at the junction point, where X−X represents the two unpaired nucleotides and the double helical arms are clockwise designated as A, B, and C. Notation and definitions of the rules proposed by Altona.[21] The TWJ is presented in its open form (center), A/B-stacked conformer, where two helices A and B are stacked with each other (left side), and A/C-stacked conformer, where two helices A and C are stacked with each other (right side), with the arrowhead pointing toward the 3′-termini and base pair symbolized by the ladder motif. Arm A penultimate positions are designated by "a" and "b". Y and R indicate pyrimidine and purine bases, respectively. To predict the preferred stacking conformer from the sequence, two empirical rules were proposed. (i) Pyrimidine rule: pyrimidine at position b favors the A/B-stacked conformer, whereas pyrimidine at position a favors the A/C-stacked conformer. (ii) Loop rule: a stable 5′-N_4/XXN_3 quasi-hairpin loop ("/" indicates break in the backbone) favors the A/B-stacked conformer, whereas a stable 5′-N_1XX/N_2 quasi-hairpin loop favors the A/C-stacked conformer. (B) Application of the extended stacking rule to the three-way junction J1, where pyrimidine at position b and a stable quasi-hairpin loop 5′-C/TTG favor the A/B-stacked conformer. (C) Application of the extended stacking rule to three-way junction J3, where pyrimidine at position a and a stable quasi-hairpin loop 5′-CTT/G favor the A/C-stacked conformer.

conformation, whereas J3 and J4 adopted the A/C-stacked conformation.[18] To confirm the generality of this observation, we studied structures J5−J11. The CD spectra from J5 to J11 (Figure S2 in Supporting Information) showed characteristic features as observed for J1−J4, with the exception of J6. For J6, an additional positive peak appeared at about 260 nm in the presence of Mg^{2+} with or without 20 wt % PEG 200. Some sequences (cf. J8−J11) also show deviation from a B-like conformation (Figure S2 in Supporting Information), but according to the rules described earlier, there should be equilibrium between the A/C- and A/B-stacked conformer. van Buuren et al. confirmed previously that there should be a deviation from the B-like geometry in the case of the A/B-stacked conformer because there was a reduced propeller twist and increased helical rise for the base pair steps near the junction for the A/B-stacked conformer in comparison with that found in the B-like conformation.[20] Our CD data support their finding because we observed that J1, J2, J6 (except in the presence of Mg^{2+}), and J7 favored A-like conformations and folded into A/B-stacked conformers, while J3, J4, and J5 favored B-like conformations and folded into A/C-stacked conformers under all conditions.

Table 1. Sequences of TWJs in This Study[a]

name	sequences	stacking conformer
J1	5′-CGTGCACCCGCTTGCGGCGACTTGTCGTTGTGCACG-3′	A/B
J2	5′-CGTGCACGCGCTTGCGCCGACTTGTCGTTGTGCACG-3′	A/B
J3	5′-CGTGCAGCGGCTTGCCGGCACTTGTGCTTCTGCACG-3′	A/C
J4	5′-CGTGCGACGGCTTGCCGGCACTTGTGCTTTCGCACG-3′	A/C
J5	5′-CGTGCAGCGGCTTGCCGGCACTTGTGCAACTGCACG-3′	A/C
J6	5′-CGTGCACCCGCTTGCGGCCACTTGTGGTTGTGCACG-3′	A/B
J7	5′-CGTGCACCCGCTTGCGGACACTTGTGTTTGTGCACG-3′	A/B
J8	5′-GCCTGCCACCGCTTGCGGTGCGTCGCTTGCGACGAAGCAGGC-3′	EQ[b]
J9	5′-GCCTGCCACCGCTTGCGGTGAGTCGCTTGCGACTAAGCAGGC-3′	EQ[b]
J10	5′-GCCTGACACCGCTTGCGGTGAGTCGCTTGCGACTAATCAGGC-3′	EQ[b]
J11	5′-GCCTGCCACCGCTTGCGGTGCGTCGCTTGCGACGTTGCAGGC-3′	EQ[b]

[a] All the unpaired nucleotides at the branch point and the tetra loops of the junctions are underlined. [b] EQ is the equilibrium mixture of A/B- and A/C-stacking conformers.

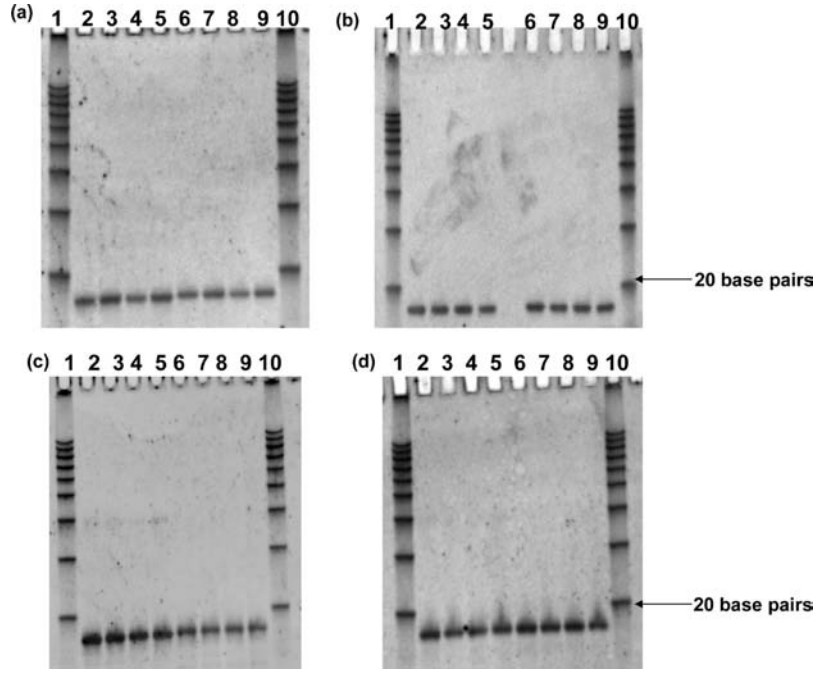

Figure 2. Nondenaturing 15% polyacrylamide gel of (a) 1 μM J1 (lanes 2−5) and 1 μM J2 (lanes 6−9), (b) 1 μM J3 (lanes 2−5) and 1 μM J4 (lanes 6−9), (c) 30 μM J1 (lanes 2−5) and 30 μM J2 (lanes 6−9), and (d) 30 μM J3 (lanes 2−5) and 30 μM J4 (lanes 6−9) in buffers of 20 mM Na-cacodylate, 0.5 mM Na_2EDTA (pH 7.0) containing 50 mM NaCl (lanes 2 and 6), 50 mM NaCl and 20 wt % PEG 200 (lanes 3 and 7), 50 mM NaCl and 5 mM $MgCl_2$ (lanes 4 and 8), and 50 mM NaCl, 5 mM $MgCl_2$, and 20 wt % PEG 200 (lanes 5 and 9) at 4 °C. Lanes 1 and 10 correspond to the 10 base pair ladder. Arrows show the bands for 20 base pairs.

These results suggest a correlation between the overall conformation of the TWJ structures and their coaxial stacking preferences.

Thermodynamics of Junction Formation. We next examined the thermal denaturation and renaturation of TWJ structures in the absence or presence of 5 mM Mg^{2+} with or without 20% PEG 200. The denaturation and renaturation curves of J1, J2, J3, and J4 traced by UV absorbance at 260 nm (Figures S3−S6 in Supporting Information, respectively) were identical under all conditions. Similar behavior was observed for all other TWJs (J5−J11) (data not shown). The melting behavior is consistent with a two-state transition between the single-strand and the TWJ structures, which allows evaluation of the thermodynamic parameters for the formation of TWJ structures. In addition, the isodichroic points observed in the CD spectra of J1 and J3 as a function of temperature also proved the two-state behavior of the melting process (Figure S7 in Supporting Information). Figure 4 shows the UV melting curves for 1 μM of J1−J4 in the absence and presence of 5 mM Mg^{2+} and 0 or 20 wt % of PEG 200. In the case of J1 (A/B-stacked TWJ), when the concentration of PEG 200 increased from 0 to 20 wt %, the average melting temperature (T_m) decreased from 60.8 to 55.6 °C in the absence of Mg^{2+} and from 69.6 to 61.7 °C in the presence of Mg^{2+} (Tables 2 and 3). A similar trend was observed with J2 (A/B-stacked TWJ), as shown in Figure 4b. In the case of J3 (A/C-stacked TWJ), the average T_m decreased from 64.1 to 55.2 °C in the absence of $Mg^{2+}$and from 67.4 to 59.8 °C in the presence of Mg^{2+} (Tables 2 and 3). J4, also an A/C-stacked TWJ, followed a similar trend (Figure 4d). For all other sequences from J5 to J11, the T_m also decreased with increasing concentrations of PEG 200 both in the absence and presence of 5 mM Mg^{2+} (data not shown). From these melting curves, thermodynamic parameters for the formation of TWJ structures were determined (Tables 2 and 3).

The stabilities ($-\Delta G°_{37}$) of the A/B- and A/C-stacked TWJs in the absence of 5 mM Mg^{2+} decreased to a similar extent (0.4 to 1.0 kcal/mol, except for J2) with increasing concentrations of PEG 200 (Table 2). On the other hand, in the presence of 5 mM Mg^{2+}, this destabilization was more pronounced for the A/B-stacked conformers as compared to

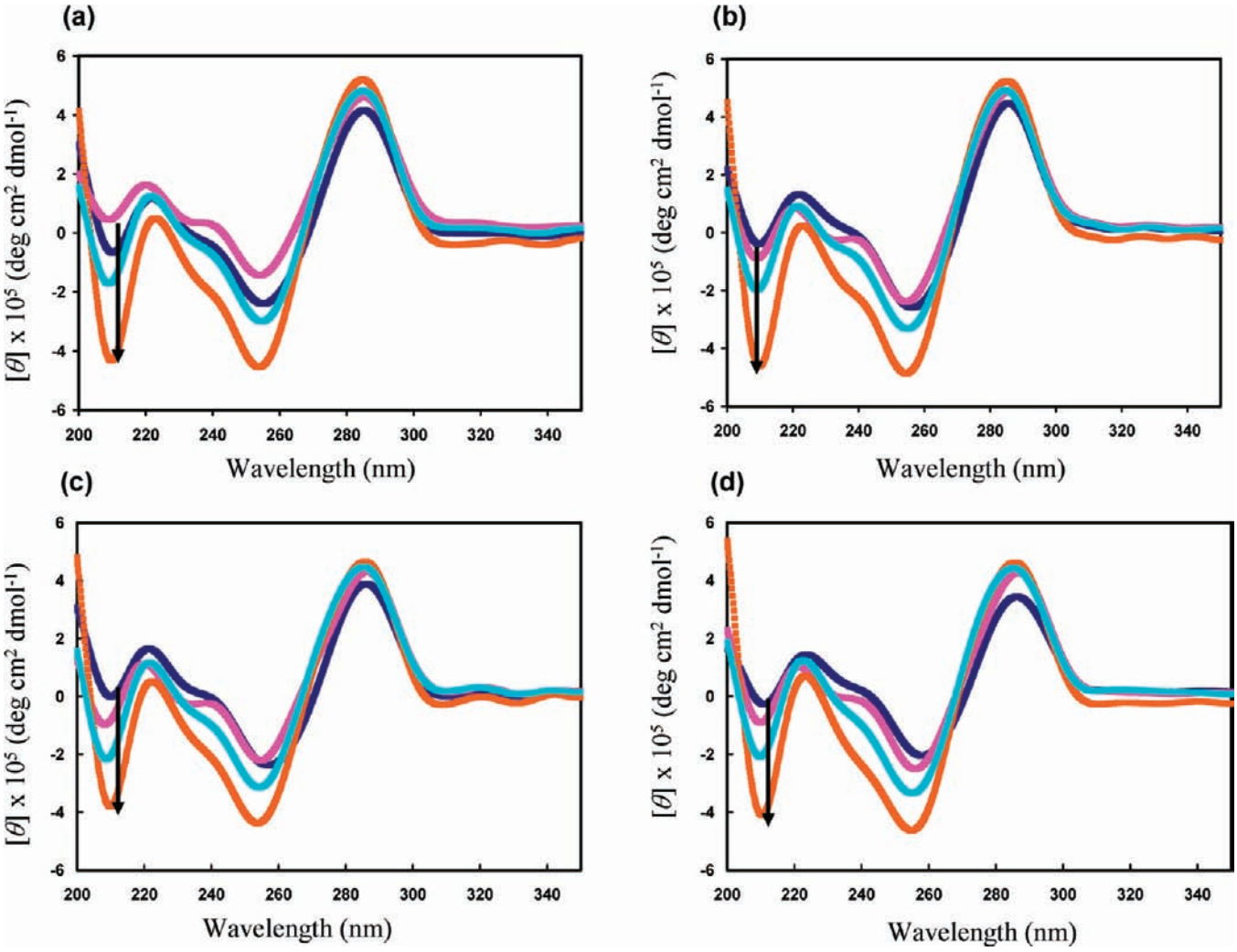

Figure 3. CD spectra of 6 μM J1 (orange), J2 (light blue), J3 (pink), and J4 (dark blue) at 4 °C in buffers of 20 mM Na-cacodylate, 0.5 mM Na_2EDTA (pH 7.0) containing (a) 50 mM NaCl, (b) 50 mM NaCl and 20 wt % PEG 200, (c) 50 mM NaCl and 5 mM $MgCl_2$, and (d) 50 mM NaCl, 5 mM $MgCl_2$, and 20 wt % PEG 200.

the A/C-stacked conformers (Table 3). In the presence of Mg^{2+}, A/B-stacked TWJs were destabilized by 1.3−1.6 kcal/mol (except for J2, which was destabilized by 0.9 kcal/mol) with increasing concentrations of PEG 200, although the A/C-stacked TWJs were destabilized only by 0.5−0.9 kcal/mol. It was previously reported that the structure of the TWJs with unpaired bases at the junction point depends on the divalent cations such as Mg^{2+}.[22] In the present study, we found that the extent of stabilization by the addition of Mg^{2+} was different for different stacking partners; A/B-stacked conformers were stabilized more than the A/C-stacked conformers by the addition of Mg^{2+}. The greater stabilization for A/B-stacked TWJs (cf. J1, J2, J6, and J7) in the presence of 5 mM Mg^{2+} was attributed to a dumbbell formation arising from end-to-end stacking of two hairpin helices (Figure 1A). On the other hand, in the case of A/C-stacked TWJs (cf. J3, J4, and J5), the hairpin helix stacks on the 5′-stem instead of end-to-end stacking with another hairpin helix (Figure 1A). This structural difference between A/B- and A/C-stacked TWJs may be the reason for lower stabilization of the A/C-stacked conformers in comparison with the A/B-stacked conformers in the presence of Mg^{2+}.

Compensation between enthalpy change and entropy change occurs in various biological systems.[23] In general, the higher-order structure formation of DNA is entropically unfavorable, whereas formation of hydrogen bonds (base pairing) and base-stacking interactions are enthalpically favored. Thermodynamic parameters in Tables 2 and 3 suggest that for A/C-stacked conformers (cf. J3, J4, and J5) the increment of Gibbs free energy with the addition of 20 wt % PEG 200 in the absence of Mg^{2+} was mostly attributed to the unfavorable enthalpic contribution (except for J3). On the other hand, in the presence of Mg^{2+}, the destabilization by 20 wt % PEG 200 was mainly due to the unfavorable entropic contribution. However, for A/B-stacked conformers (cf. J1, J2, J6, and J7), the changes in the enthalpy and entropy values were totally opposite. In the absence of Mg^{2+}, unfavorable entropy change was responsible for the decreased stability of the A/B-stacked TWJ structures with an increased concentration of PEG 200 (except for J6). On the other hand, in the presence of Mg^{2+}, unfavorable enthalpic change was responsible for the decreased stability of the TWJ structure with 20 wt % PEG 200 (except for J2). Zhong et al. observed large hydration changes accompanying the junction formation

(23) Marky, L. A.; Kupke, D. W. *Methods Enzymol.* **2000**, *323*, 419–441.

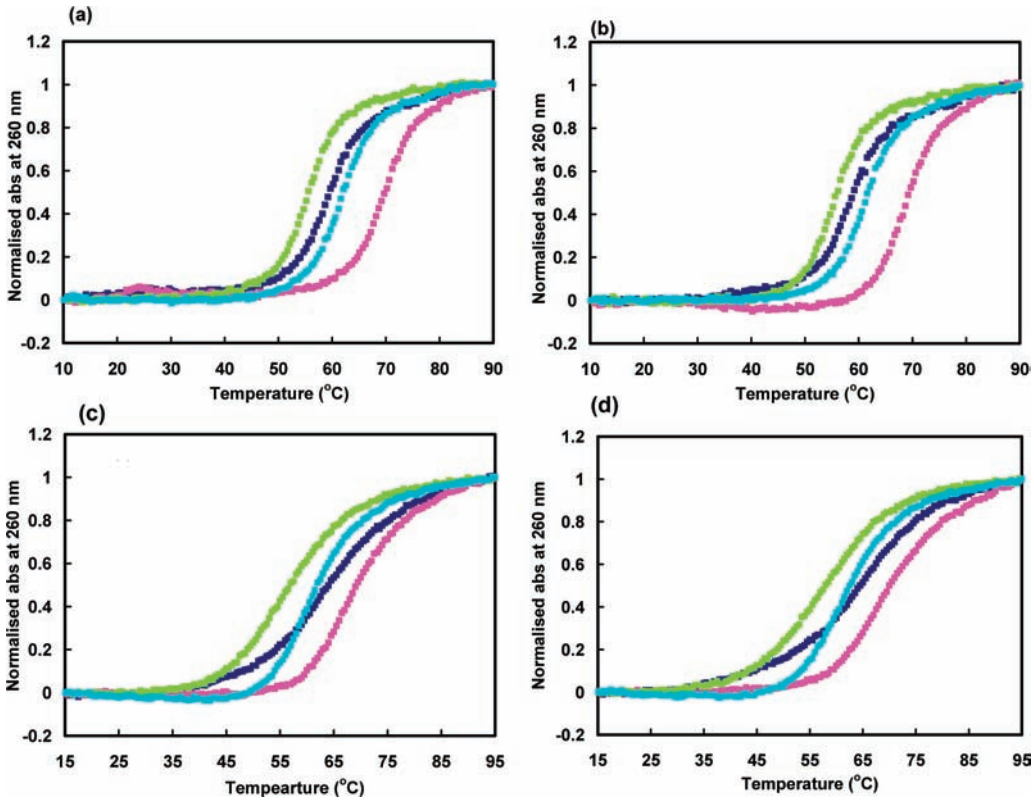

Figure 4. Normalized UV melting curves for 1 μM of (a) J1, (b) J2, (c) J3, and (d) J4 in buffers of 20 mM Na-cacodylate, 0.5 mM Na_2EDTA (pH 7.0) containing 50 mM NaCl (dark blue), 50 mM NaCl and 20 wt % PEG 200 (green), 50 mM NaCl and 5 mM $MgCl_2$ (pink), and 50 mM NaCl, 5 mM $MgCl_2$, and 20 wt % PEG 200 (light blue). Melting was assessed by UV absorbance at 260 nm and a melting rate of 0.5 °C/min.

Table 2. Thermodynamic Parameters for the Formation of TWJ with 50 mM NaCl[a]

ionic condition	stacking conformer	DNA	PEG 200 (wt %)	T_m (°C)	$\Delta G°_{37}$ (kcal/mol)	$T\Delta H°$ (kcal/mol)	$\Delta S°$ (cal/mol/K)
Na^+	A/B-stacked conformer	J1	0	60.8 ± 1.3	−3.7 ± 0.2	−52.3 ± 1.8	−156.7 ± 5.6
			20	55.6 ± 0.4	−3.1 ± 0.1	−54.3 ± 2.6	−165.2 ± 7.9
		J2	0	57.8 ± 0.4	−3.4 ± 0.2	−54.0 ± 2.3	−164.0 ± 6.7
			20	55.3 ± 0.2	−3.3 ± 0.1	−60.0 ± 1.8	−182.0 ± 5.4
		J6	0	58.5 ± 0.3	−3.7 ± 0.2	−56.7 ± 3.2	−171.1 ± 9.8
			20	54.8 ± 0.2	−3.0 ± 0.1	−55.2 ± 1.4	−168.4 ± 4.4
		J7	0	55.8 ± 0.9	−2.9 ± 0.4	−50.5 ± 5.4	−153.5 ± 15.9
			20	52.8 ± 1.1	−2.5 ± 0.3	−51.4 ± 3.7	−157.6 ± 11.0
	A/C-stacked conformer	J3	0	64.1 ± 0.4	−2.5 ± 0.1	−31.3 ± 0.5	−92.9 ± 1.3
			20	55.2 ± 0.8	−1.9 ± 0.1	−33.9 ± 1.2	−102.9 ± 3.8
		J4	0	66.5 ± 0.7	−3.0 ± 0.2	−35.0 ± 3.6	−102.0 ± 11
			20	58.4 ± 0.3	−2.0 ± 0.1	−30.0 ± 1.0	−92.0 ± 3.1
		J5	0	63.2 ± 2.8	−2.8 ± 0.1	−36.6 ± 4.0	−108.8 ± 12.9
			20	56.9 ± 0.7	−2.1 ± 0.1	−34.9 ± 1.9	−105.7 ± 5.4
	mixtureof A/B- and A/C-stacked conformers	J8	0	64.6 ± 0.5	−3.0 ± 0.1	−37.0 ± 0.4	−109.0 ± 1.2
			20	61.4 ± 0.5	−3.4 ± 0.1	−46.0 ± 0.8	−137.0 ± 2.3
		J9	0	65.6 ± 2.5	−2.8 ± 0.3	−33.0 ± 2.2	−97.5 ± 6.0
			20	60.0 ± 0.7	−2.9 ± 0.3	−41.5 ± 4.1	−124.6 ± 12.3
		J10	0	56.5 ± 2.8	−1.6 ± 0.3	−29.4 ± 4.6	−87.6 ± 11.2
			20	53.3 ± 1.8	−1.7 ± 0.3	−34.8 ± 7.6	−106.6 ± 23.8
		J11	0	63.5 ± 1.4	−2.7 ± 0.3	−34.6 ± 1.5	−102.9 ± 4.0
			20	62.8 ± 2.2	−3.2 ± 0.3	−41.5 ± 1.9	−123.6 ± 5.4

[a] All the experiments were carried out in buffers containing 20 mM sodium-cacodylate, 0.5 mM Na_2EDTA, 50 mM NaCl with 0 and 20 wt % PEG 200. Thermodynamic parameters are the average values obtained from melting curves with concentration range from 0.5 to 30 μM of DNA oligonucleotides.

in comparison with the duplex formation.[8c] They also pointed out that the states of hydration for the duplex and TWJ states were quite different from each other. In the present study, all TWJs were destabilized with an increased concentration of PEG 200 from 0 to 20 wt % both in the absence and presence of Mg^{2+}, suggesting hydrations during their formation.[14b] However, the molecular crowding effect on the junction point of the TWJ is still unclear since all duplex arms of the TWJ should also be destabilized by molecular crowding conditions.[14b] To reveal the state of hydration at the junction point, we next compared the states of hydration of the whole TWJ structure and each helical duplex arm.

Hydration of the TWJ Structures. TWJs consist of three helical arms and a junction point where all three helices meet.

Table 3. Thermodynamic Parameters for the Formation of TWJ with 50 mM NaCl and 5 mM $MgCl_2$[a]

ionic condition	stacking conformer	DNA	PEG 200 (wt %)	T_m (°C)	$\Delta G°_{37}$ (kcal/mol)	$\Delta H°$ (kcal/mol)	$\Delta S°$ (cal/mol/K)
Na^+ and Mg^{2+}	A/B-stacked conformer	J1	0	69.6 ± 0.8	−5.6 ± 0.3	−58.7 ± 2.6	−171.1 ± 7.4
			20	61.7 ± 0.6	−4.1 ± 0.1	−55.1 ± 1.8	−164.6 ± 5.7
		J2	0	68.6 ± 0.3	−5.0 ± 0.1	−55.0 ± 1.6	−160.0 ± 4.7
			20	60.8 ± 0.1	−4.1 ± 0.1	−57.0 ± 0.9	−170.0 ± 2.7
		J6	0	69.7 ± 0.2	−5.7 ± 0.3	−60.2 ± 3.5	−175.6 ± 10.4
			20	62.5 ± 0.4	−4.1 ± 0.4	−54.1 ± 5.4	−161.3 ± 16.4
		J7	0	66.5 ± 0.6	−4.5 ± 0.1	−51.7 ± 2.5	−152.1 ± 7.5
			20	59.9 ± 1.1	−3.2 ± 0.1	−46.7 ± 1.4	−140.2 ± 4.7
	A/C-stacked conformer	J3	0	67.4 ± 0.4	−4.0 ± 0.2	−45.4 ± 2.4	−133.3 ± 7.1
			20	59.8 ± 0.2	−3.1 ± 0.1	−45.6 ± 0.3	−136.9 ± 1.0
		J4	0	67.8 ± 0.7	−3.7 ± 0.3	−41.0 ± 3.5	−119.0 ± 10.4
			20	60.9 ± 0.3	−3.1 ± 0.1	−44.0 ± 1.5	−131.0 ± 4.6
		J5	0	66.3 ± 1.7	−3.1 ±0.2	−35.7 ± 1.5	−105.1 ± 5.4
			20	60.5 ± 0.6	−2.6 ± 0.1	−36.6 ± 0.9	−109.6 ± 2.9
	mixture of A/B- and A/C-stacked conformer	J8	0	74.5 ± 0.8	−5.1 ± 0.2	−47.0 ± 0.7	−136.0 ± 1.7
			20	66.4 ± 0.4	−4.6 ± 0.1	−53.0 ± 1.3	−157.0 ± 3.8
		J9	0	72.8 ± 1.4	−4.6 ± 0.3	−43.5 ± 3.7	−125.5 ± 11.0
			20	64.9 ± 0.6	−3.9 ± 0.3	−46.8 ± 2.1	−138.5 ± 6.2
		J10	0	68.8 ± 0.7	−2.9 ± 0.2	−30.6 ± 2.5	−89.5 ± 7.1
			20	60.2 ± 1.0	−2.8 ± 0.4	−40.7 ± 6.3	−122.1 ± 19.3
		J11	0	77.4 ± 0.5	−5.6 ± 0.4	−48.6 ± 3.4	−138.6 ± 9.7
			20	69.8 ± 2.0	−4.6 ± 0.2	−53.2 ± 3.5	−140.5 ± 10.9

[a] All the experiments were carried out in buffers containing 20 mM sodium-cacodylate, 0.5 mM Na_2EDTA, 50 mM NaCl, and 5 mM $MgCl_2$ with 0 and 20 wt % PEG 200. Thermodynamic parameters are the average values obtained from melting curves with concentration range from 0.5 to 30 μM of DNA oligonucleotides.

The overall effect of the molecular crowding condition of cosolutes, such as PEG 200, on the whole TWJ structure can be divided into the effects on the junction point as well as on the duplex arms. It was shown that indirect interactions of cosolutes such as PEG 200 with DNA structures affected the thermodynamics of the DNA structures by regulating the hydration of the DNA molecule.[11a] In this way, molecular crowding with PEG 200 can alter the stability of the TWJs by modulating their state of hydration. To determine the state of hydration at the junction point of the TWJs, we must quantify the water molecules associated with the whole TWJ and all helical arms. We have selected two representative examples, J1 (A/B-stacked TWJ) and J3 (A/C-stacked TWJ), to estimate the hydration in each case. We estimated the thermodynamic parameters ($\Delta H°$, $\Delta S°$, and $\Delta G°_{37}$) for the formation of J1 and J3 in the presence of various concentrations of PEG 200. Table S1 in Supporting Information shows the values of $\Delta H°$, $\Delta S°$, and $\Delta G°$ at 37 °C for the formation of structures as well as the water activities with various concentrations of PEG 200 from 0 to 40 wt % (Figure 5a,b for J1 and Figure S8 in Supporting Information for J3) in the absence and presence of 5 mM Mg^{2+}.

Formation of an intramolecular structure by a DNA strand in an aqueous solution containing neutral cosolute (PEG 200) and a cation can be represented as follows:

$$A_{ss} \rightleftharpoons A_f + \Delta n_w H_2O + \Delta n_{cs} CS + \Delta n_{M^+} M^+ \qquad (1)$$

where A_{ss} and A_f represent single-stranded and formed DNA structures, respectively; CS is the cosolute; M^+ is a cation; and Δn_w, Δn_{cs}, and Δn_{M^+} are the numbers of water, cosolute, and cation, respectively, released upon formation of the structures.[24,14b] At constant temperature and pressure, the derivative of ln K_{obs} by ln a_w is represented by eq 2.[11a,14b]

$$\frac{d \ln K_{obs}}{d \ln a_w} = \left[\Delta n_w + \Delta n_{cs}\left(\frac{d \ln a_{cs}}{d \ln a_w}\right) + \Delta n_{M^+}\left(\frac{d \ln a_{M^+}}{d \ln a_w}\right)\right] \qquad (2)$$

In the present study, Δn_w, Δn_{cs}, and Δn_{M^+} are the numbers of water molecules, cosolute (PEG 200), and Na^+ or Mg^{2+}, respectively, released upon the formation of the TWJ structure or each hairpin duplex arm. The dependence of equilibrium constant (ln K_{obs}) on water activity (ln a_w), as determined by osmotic pressure measurements at 37 °C for J1 and J3, is shown in Figure 5c. The plot reveals that, both in the absence and presence of 5 mM Mg^{2+}, the stability of the TWJ structure in terms of the observed equilibrium constant (ln K_{obs}) increases linearly with the increase of water activity (ln a_w). The linearity of the plots suggests that the variable terms in eq 2 are negligible and the slope of the curves is approximately equal to the constant term, $-\Delta n_w$.[11a,14b] The slopes of the plot in Figure 5c for J1 and J3 in the absence and presence of Mg^{2+} provide positive values of $-\Delta n_w$, leading to the uptake of water molecules during the formation of TWJ structures. Notably, in our present study, the thermal stability term (ln K_{obs}) was needed for the estimation of the number of water molecules (Δn_w) associated with the structure formation. It has been reported that, in spite of the clear temperature dependence of the enthalpy or entropy changes ($\Delta H°$ or $\Delta S°$), the free energy change ($\Delta G°$) is relatively insensitive to the heat capacity change. This suggests that the free energy change determined by spectroscopic technique with the assumption $\Delta C_p = 0$ is an accurate parameter for the estimation of Δn_w.

The numbers of water molecules taken up during the formation of J1 and J3 in the absence of Mg^{2+} were estimated to be 38.3 and 25.0, respectively, and those in the presence of Mg^{2+} were estimated to be 63.2 and 48.5, respectively. Next, we estimated the number of water molecules associated with the hairpin duplex arms. The hairpin duplex arms, J1-AB and J1-C for J1, and J3-AC and J3-B for J3, are shown in Figure 6a,b. The formation of these duplex arms was further confirmed by native PAGE and CD spectra (Figure S9 and S10 in Supporting Information). The plots of ln K_{obs} for the formation of hairpin duplexes at 37 °C versus ln a_w in Figure 6c,d also are linear with increasing water activity. Similarly, the numbers of water molecules taken up by the two arms (J1-C and J1-

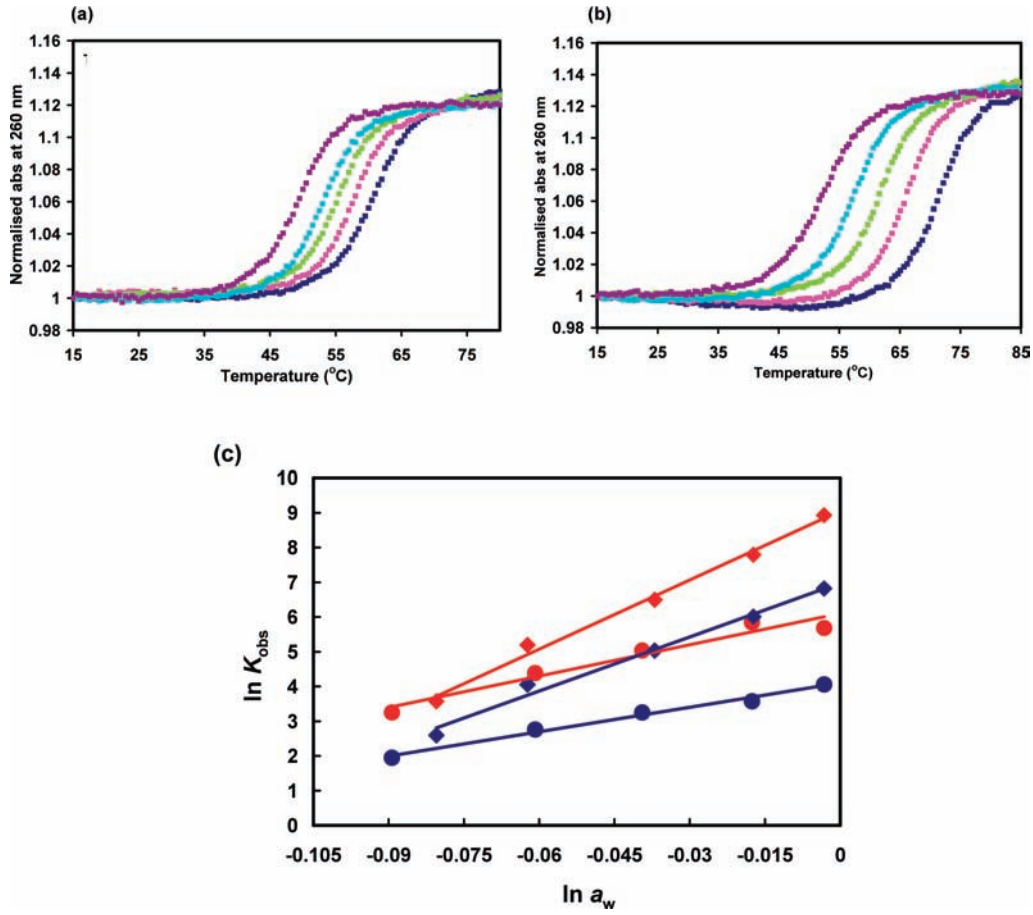

Figure 5. (a) Normalized UV melting curves for 1 μM J1 in the presence of 50 mM NaCl, and (b) normalized UV melting curves for 1 μM J1 in the presence of 50 mM NaCl and 5 mM $MgCl_2$ in buffers of 20 mM Na-cacodylate, 0.5 mM Na_2EDTA (pH 7.0) containing 0 wt % (dark blue), 10 wt % (pink), 20 wt % (green), 30 wt % (light blue), and 40 wt % (purple) of PEG 200. Melting was assessed by UV absorbance at 260 nm and a heating rate of 0.5 °C /min. (c) Plots of ln K_{obs} versus ln a_w for the formation of J1 (red) and J3 (blue) in buffers of 20 mM Na-cacodylate, 0.5 mM Na_2EDTA (pH 7.0) containing 50 mM NaCl (circle), and 50 mM NaCl and 5 mM $MgCl_2$ (square) at 37 °C.

AB) of J1 in the absence of Mg^{2+} were estimated to be 43.7 and 48.0, respectively, and those in the presence of Mg^{2+} were estimated to be 52.5 and 66.9, respectively. The number of water molecules taken up for the formation of two arms (J3-AC and J3-B) of J3 were estimated to be 38.5 and 36.3 in the absence of Mg^{2+} and 78.2 and 48.4 in the presence of Mg^{2+}, respectively (Table S2 in Supporting Information). These quantitative results demonstrate the hydration of the whole TWJ structures as well as the duplex arms during their formation. Notably, the extents of hydration for the whole TWJs and each duplex arm were quite different both in the absence and presence of Mg^{2+}. The total number of water molecules taken up by the duplex arms was significantly higher than that of the whole TWJ structures. If the combination of J1-C and J1-AB would give rise to J1, and that of J3-AC and J3-B would give rise to J3, then it would be possible to determine the effect of molecular crowding on the junction point of the TWJ from their differential state of hydration. The differential values ($\Delta\Delta n_w$) for J1 and J3 [where $\Delta\Delta n_w = (-\Delta n_w$ for the whole junction$) - (-\Delta n_w$ for all the duplex arms)] was found to be negative (Table S2 in Supporting Information), suggesting the release of water molecules from the junction point of the TWJ structure under all conditions. The dehydration from the junction point of the TWJ structure was also verified by other sets of the duplex arms of J1 and J3 (Figure S11 in Supporting Information). The number of water molecules taken up by the duplex arms ($-\Delta n_w$) and the differential number of water molecules ($\Delta\Delta n_w$) are also listed in Table S2. It was evident from the NMR study that the interhelix angle in the TWJ (53°) was less sharp than that in the four-way junction crystal structure (40°).[20] The discovery of a new mode of DNA recognition has revealed that a TWJ of DNA can be a potential structural target for highly specific drugs due to the presence of a hydrophobic core at the junction point of the TWJ.[25] Thus, there must be partial exposure of the aromatic groups to the solvents due to the opening of bases at the junction point. Moreover, a spine of hydration, that is a network of water molecules, observed in grooves in the duplex structure, cannot be formed at the junction point. These structural properties of the junction can lead to the release of water molecules. From these results, we conclude that molecular crowding conditions favor the formation of less hydrated TWJ structures in comparison with the duplex formation.

Regulation of the Duplex-Junction Transition. To explore the stabilization of the TWJ structures in comparison with the duplexes by molecular crowding conditions, we designed short DNA sequences that can form an intermolecular duplex along with the TWJ structure under a dilute condition. A crowding agent that can modulate DNA hydration will differentially affect

(24) (a) Spink, C. H.; Chaires, J. B. *Biochemistry* **1999**, *38*, 496–508. (b) Goobes, R.; Kahana, N.; Cohen, O.; Minsky, A. *Biochemistry* **2003**, *42*, 2431–2440.
(25) Oleksi, A.; Blanco, A. G.; Boer, R.; Uson, I.; Aymami, J.; Rodger, A.; Hannon, M. J.; Coll, M. *Angew. Chem., Int. Ed.* **2006**, *45*, 1227–1231.

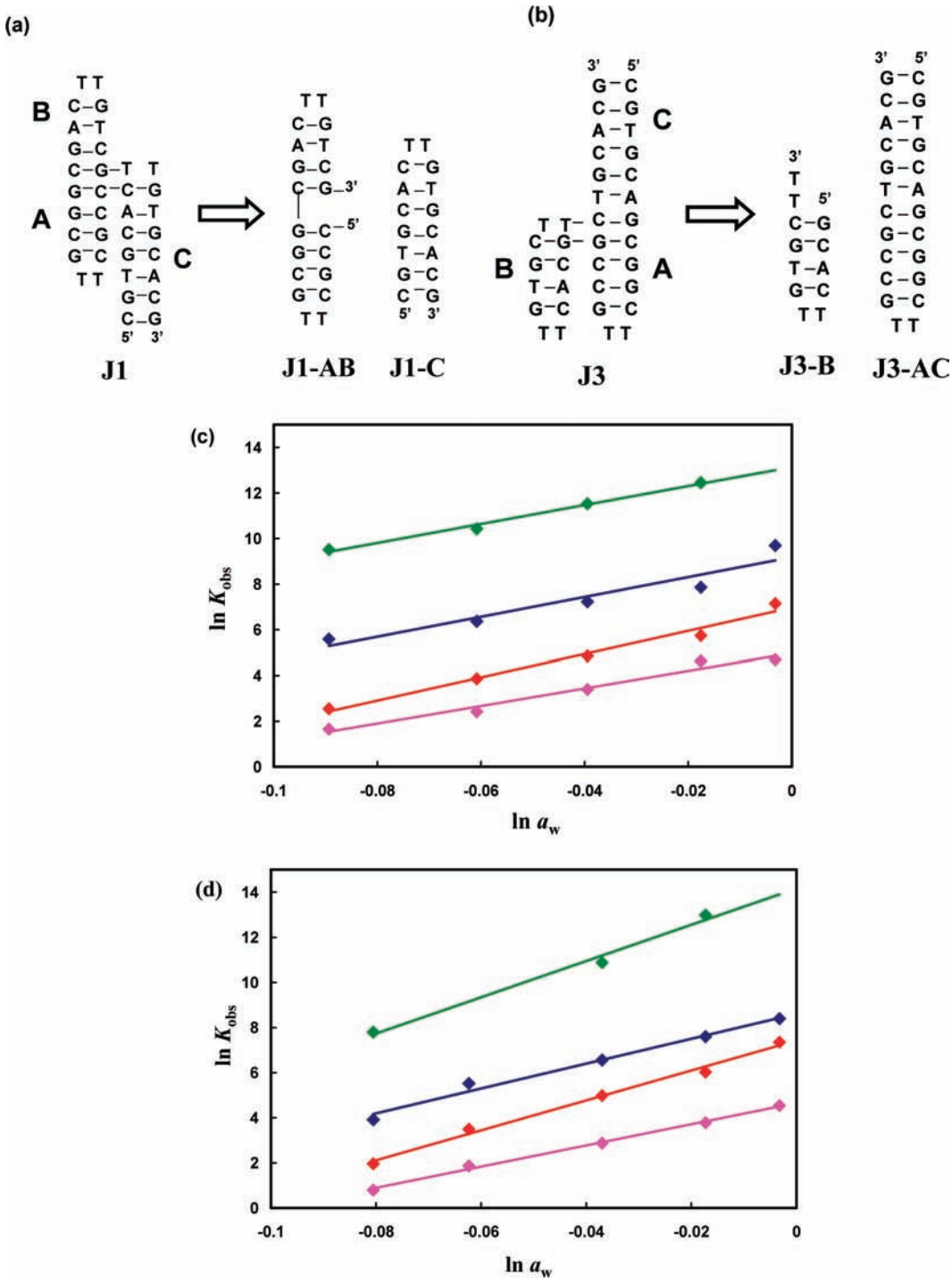

Figure 6. Schematic representation of the two individual arms, (a) J1-C and J1-AB of the A/B-stacked junction J1, and (b) J3-AC and J3-B of the A/C-stacked junction J3. Plots of ln K_{obs} versus ln a_w for the formation of J1-C (blue), J1-AB (red), J3-AC (green), and J3-B (pink) in buffers of 20 mM Na-cacodylate, 0.5 mM Na_2EDTA (pH 7.0) containing (c) 50 mM NaCl and (d) 50 mM NaCl and 5 mM $MgCl_2$ at 37 °C.

the structure and stability of the DNA motifs. Differential hydration may lead to the structural transition from more hydrated to less hydrated DNA structures.[26] From this point of view, we have designed DNA sequences from J12 to J15 (Figure 7a) by truncating the A and B arms of J8. Figure 7b−e shows a 15% native PAGE of 1 and 30 μM concentration of J12−J15 in the absence and presence of 5 mM Mg^{2+} with 0 or 20 wt % of PEG 200 at 4 °C.

Native PAGE experiments with 1 and 30 μM of J12 and J13 (Figure 7b,d) show that both sequences form only the TWJ structure under all conditions because their migration is consistent with 16 and 14 base pair formations, respectively. However, for J14 (Figure 7c), two bands were found under all conditions with the 1 μM concentration. Migration of the upper band was consistent with a 30 base pair band of a 10 base pair ladder marker and indicated the formation of a duplex. The faster migrating band was for a TWJ with 12 base pair formation. When the concentration of J14 was increased from 1 to 30 μM,

(26) Preisler, R. S.; Chen, H. H.; Colombo, M. F.; Choe, Y.; Short, B. J., Jr.; Rau, D. C. *Biochemistry* **1995**, *34*, 14400–14407.

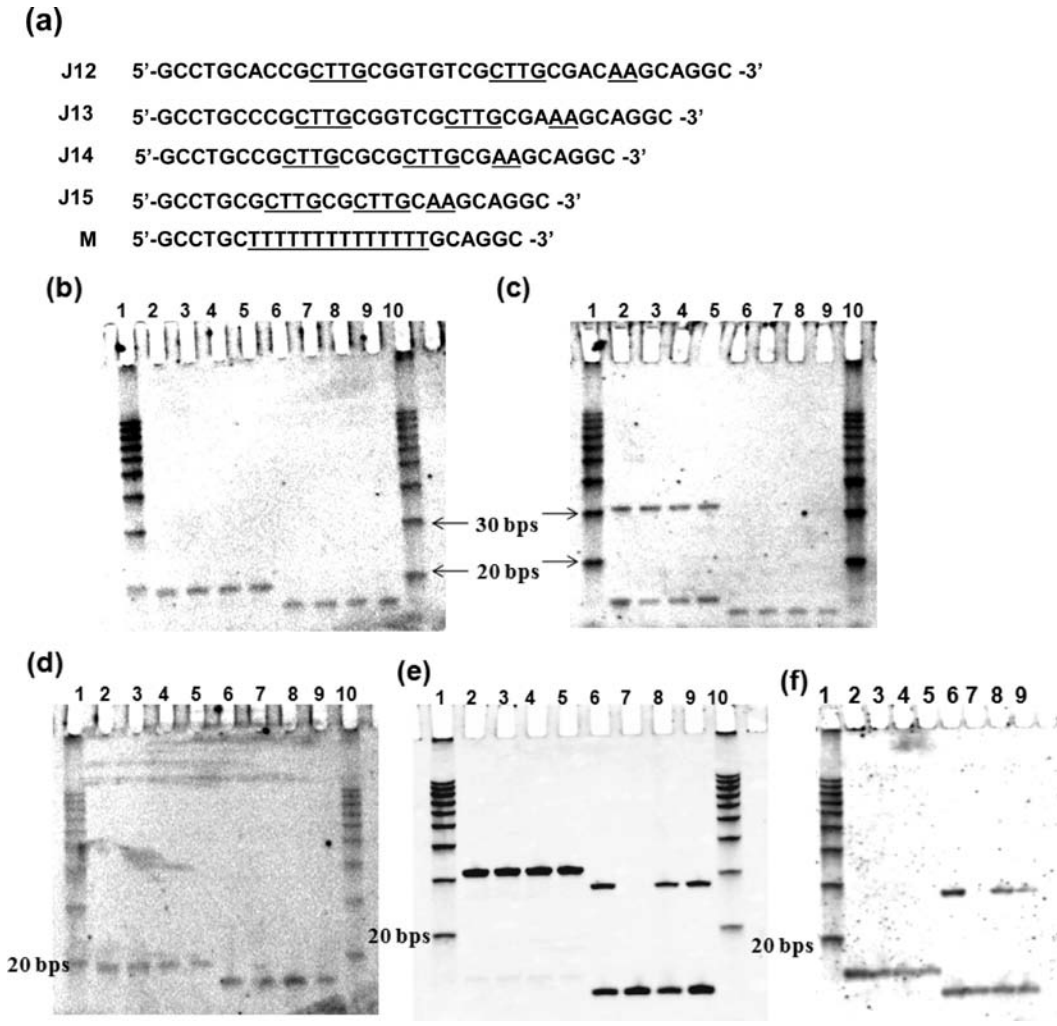

Figure 7. (a) Sequences of the truncated TWJs and their abbreviations. The underlines indicate the terminal loops and the unpaired nucleotides at the junction point. Nondenaturing 15% polyacrylamide gel of (b) 1 μM J12 (lanes 2−5) and 1 μM J13 (lanes 6−9), (c) 1 μM J14 (lanes 2−5) and 1 μM J15 (lanes 6−9), (d) 30 μM J12 (lanes 2−5) and 30 μM J13 (lanes 6−9), (e) 30 μM J14 (lanes 2−5) and 30 μM J15 (lanes 6−9) and (f) 30 μM M (lanes 2−5) and 30 μM J15 (lanes 6−9) in buffers of 20 mM Na-cacodylate, 0.5 mM Na_2EDTA (pH 7.0) containing 50 mM NaCl (lanes 2 and 6), 50 mM NaCl and 20 wt % PEG 200 (lanes 3 and 7), 50 mM NaCl and 5 mM $MgCl_2$ (lanes 4 and 8), and 50 mM NaCl, 5 mM $MgCl_2$, and 20 wt % PEG 200 (lanes 5 and 9) at 4 °C. Lanes 1 and 10 correspond to the 10 base pair ladder. Arrows show the bands for 20 and 30 base pairs.

the native PAGE exhibited only the upper band for the bimolecular duplex (Figure 7e).

Native PAGE experiments with J15 also exhibited two bands with the 30 μM concentration (Figure 7e). The upper band migrated slightly faster than the 30 base pair band of the 10 base pair ladder marker, indicating the formation of a bimolecular duplex, and the lower band showed a TWJ formation with 10 base pairs. Formation of the TWJ structure was confirmed by the use of marker DNA (M) having the same length as J15 and a large loop replacing arms A and B (Figure 7f). In the case of J15, it was interesting to observe that, in the absence of Mg^{2+}, the addition of 20 wt % PEG 200 eliminated the duplex formation and induced the formation of a TWJ structure (Figure 7e). On the other hand, in the presence of Mg^{2+}, this structural change was not prominent.

We also performed native PAGE experiments with varying concentrations of J15 under all conditions and with 30 μM of J15 with an increased concentration of PEG 200 from 0 to 30 wt % both in the absence and presence of 5 mM Mg^{2+} (Figure 8). In the absence of Mg^{2+}, all concentrations of J15 (except for 1 μM) exhibited two bands under the dilute condition (Figure 8a). Addition of 20 wt % PEG 200 eliminated the formation of the slower migrating band (bimolecular duplex) and induced the formation of the faster migrating band containing the TWJ structure. On the contrary, Figure 8b shows that the duplex-junction transition cannot be effectively regulated with the addition of 20 wt % PEG 200 in the presence of Mg^{2+}. Furthermore, the native PAGE experiment with the 30 μM concentration of J15 (Figure 8c) revealed an increase in the fraction of TWJ structures with the increased concentration of PEG 200 from 0 to 30 wt % in the absence of Mg^{2+}. In the presence of Mg^{2+}, the fraction of TWJ structures did not change effectively with increasing concentrations of PEG 200 (Figure 8d). Figure 8e shows the clear dependence of the PEG 200 concentration on the duplex-junction transition at 4 °C in the absence of Mg^{2+}, although no significant dependency of the PEG 200 concentration was observed for such duplex-junction transition in the presence of Mg^{2+} (Figure 8f).

Stabilization of the bimolecular duplex by a divalent cation such as Mg^{2+} in comparison with Na^+ is a possible reason for this observation.[27] Our group reported that the hairpin−duplex

(27) Nakano, S.; Fujimoto, M.; Hara, H.; Sugimoto, N. *Nucleic Acids Res.* **1999**, *27*, 2957–2965.

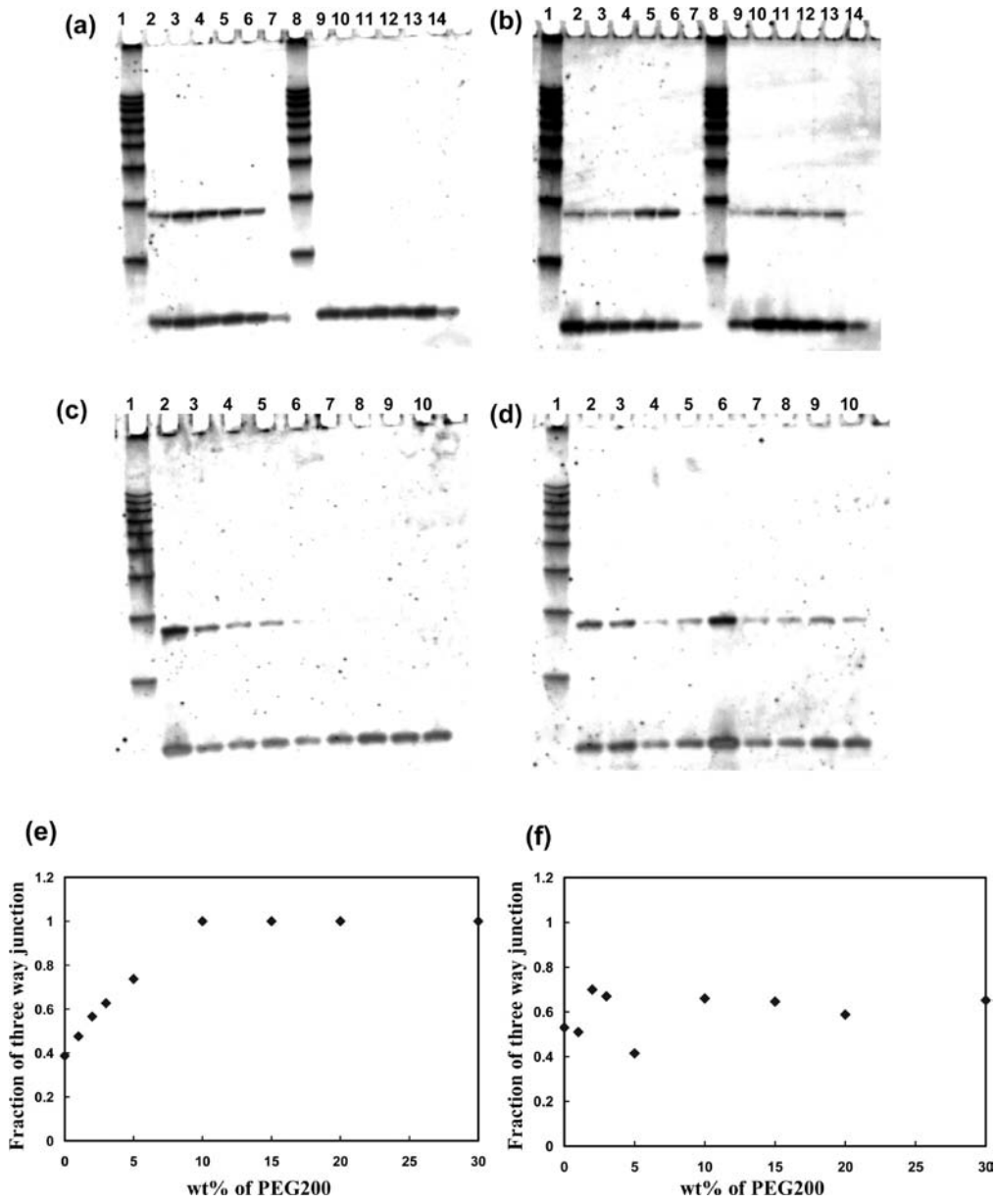

Figure 8. Nondenaturing 15% polyacrylamide gel of J15 in buffers of 20 mM Na-cacodylate, 0.5 mM Na_2EDTA (pH 7.0) containing (a) 50 mM NaCl (lanes 2−7) and 50 mM NaCl and 20 wt % PEG 200 (lanes 9−14), (b) 50 mM NaCl and 5 mM $MgCl_2$ (lanes 2−7), and 50 mM NaCl, 5 mM $MgCl_2$, and 20 wt % PEG 200 (lanes 9 and 14) at 4 °C with various concentrations of DNA such as 30, 20, 15, 10, 5, and 1 μM (lanes 2−7 and lanes 9−14). Lanes 1 and 8 correspond to the 10 base pair ladder. Nondenaturing 15% polyacrylamide gel of J15 in buffers of 20 mM Na-cacodylate, 0.5 mM Na_2EDTA (pH 7.0) containing (c) 50 mM NaCl, and (d) 50 mM NaCl and 5 mM $MgCl_2$ with various concentrations of PEG200 from 0 to 30 wt % at 4 °C. Lanes 2−10 correspond to increasing concentrations of PEG 200 from 0, 1, 2, 3, 5, 10, 15, 20, to 30 wt %. Lane 1 corresponds to the 10 base pair ladder. Dependence of the fraction of TWJ (J15) on varying concentrations of PEG 200 in buffers of 20 mM Na-cacodylate, 0.5 mM Na_2EDTA (pH 7.0) containing (e) 50 mM NaCl and (f) 50 mM NaCl and 5 mM $MgCl_2$ at 4 °C.

equilibrium could be shifted to the bimolecular duplex with increasing concentrations of cationic molecules including Mg^{2+}.[28] This structural change from the hairpin loop to the duplex induced by Mg^{2+} was due to favorable cation binding to the duplex, according to the polyelectrolyte theory.[29] In contrast to the previous result, we successfully achieved a structural transition from the bimolecular duplex to the unimolecular TWJ structure with increasing concentrations of PEG 200 (Figure 9). Therefore, it is very interesting to conclude from our present results that molecular crowding conditions were much more effective for assisting the formation of the TWJ structure in comparison with Mg^{2+} because molecular crowding stabilizes the junction points of TWJ structures and destabilizes the duplexes, whereas Mg^{2+} stabilizes both the structures.

Biological Significance. There is extensive need for thermodynamic data for rational design of molecules functioning inside cells as well as for better understanding of biological processes inside cells. However, most thermodynamic data were obtained from in vitro evaluations using a homogeneous aqueous solution, while molecular crowding is one of the most important differences between in vivo and in vitro conditions. Although some of the characters of PEG are very different from that of

(28) Nakano, S.; Kirihata, T.; Sugimoto, N. *Chem. Commun.* **2008**, 700–702.
(29) Record, M. T., Jr; Anderson, C. F.; Lohman, T. M. *Q. Rev. Biophys.* **1978**, *2*, 103–178.

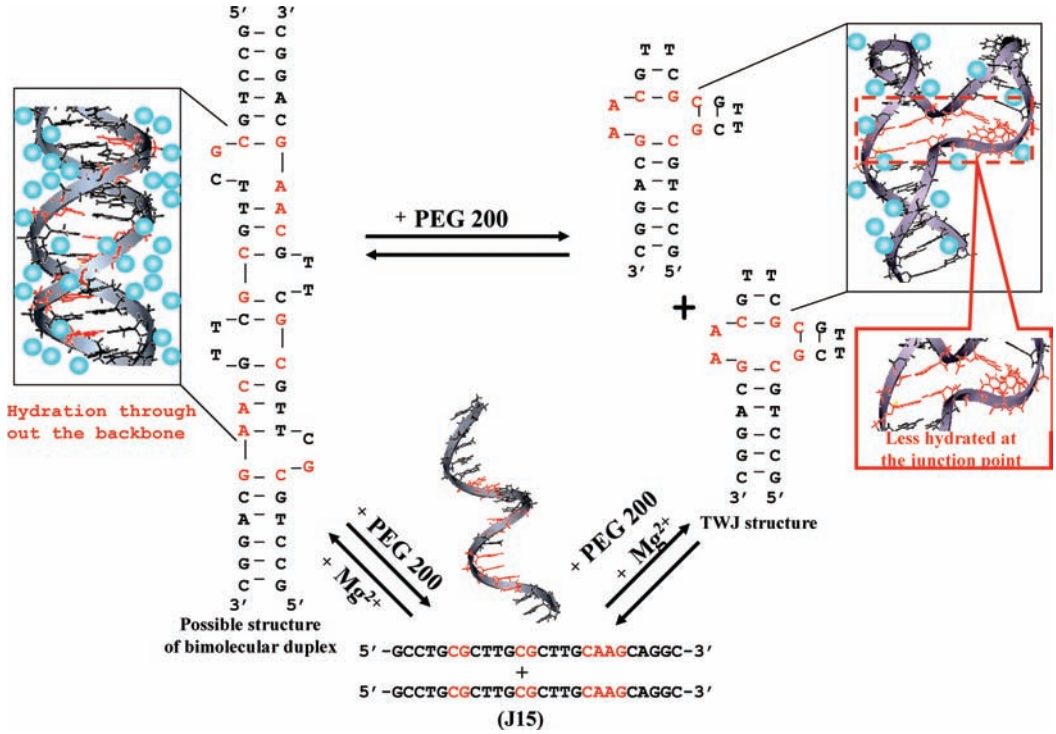

Figure 9. Schematic representation of duplex-junction transition along with the single strand under molecular crowding conditions illustrating the significance of hydration of the TWJ structure. Blue circles indicate the water molecules. Bases at the junction point are marked with red.

proteins which is the most abundant biomolecules inside cells, it is notable that the use of PEG as molecular crowding agent can give quantitative information that is critical to predict behaviors of biomolecules under various conditions including cell mimicking. In this regards, our present study of the TWJs of DNA can provide valuable quantitative information regarding the thermodynamics and hydration of the branch site affected by the water activity.

Additionally, it is well-known that divalent metal ions, such as Mg^{2+}, are generally required for the stabilization of TWJs of DNA. Moreover, Mg^{2+} is thought to be important for rapid folding of nucleotide sequences because it can stabilize native folding motifs and allow packing of the negatively charged phosphate backbone. However, there are a number of ways in which Mg^{2+} could also slow the folding of such DNA or RNA structural motifs.[30a] There is evidence that high Mg^{2+} concentrations can unfavorably reshape the folding pathway by stabilizing an off-pathway intermediate that must unfold before completion of the native structure formation.[30] Therefore, an optimal concentration of Mg^{2+} is required for correct folding and stabilization of such structural motifs. Most of the Mg^{2+}-dependent in vitro studies of different RNA or DNA structural motifs used relatively high concentrations of Mg^{2+} (5−10 mM), while in vivo concentrations of Mg^{2+} are as low as 1 mM, but the factors involved in folding of DNA or RNA structural motifs at such a low intracellular Mg^{2+} concentration were not well understood. Our findings highlight the significance of the alteration of hydration in crowded environments. Molecular crowding can associate intramolecular TWJs, which are frequently observed in high-order structures of nucleic acids. These findings emphasize the importance of molecular crowding in the intracellular environment to support the correct folding and protect nucleic acids from improper intermolecular associations, even at a very low concentration of Mg^{2+}. This chaperon-like function of molecular crowding is also useful to maintain the activities of various functional nucleic acids that play pivotal roles both in vivo and in vitro.

Acknowledgment. This work was supported in part by Grants-in-Aid for Scientific Research, the "Core research" project (2009−2014), and the "Academic frontier" project (2004−2009) from the Ministry of Education, Culture, Sports, Science and Technology, Japan, the Hirao Taro Foundation of the Konan University Association for Academic Research, and the Long-Range Research Initiative Project of Japan Chemical Industry Association.

Supporting Information Available: Additional figures and tables. This material is available free of charge via the Internet at http://pubs.acs.org.

JA900744E

(30) (a) Rook, M. S.; Treiber, D. K.; Williamson, J. R. *Proc. Natl. Acad. Sci. U.S.A.* **1999**, *96*, 12471–12476. (b) Pan, J.; Thirumalai, D.; Woodson, S. A. *Proc. Natl. Acad. Sci. U.S.A.* **1999**, *96*, 6149–6154.